b_1, b_2	parameter in the Fuoss equation for the pure components
c	concentration of the undissociated electrolyte solute
c_+, c_-	concentration of the electrolyte ions
e	4.803×10^{-10} esu
f_1', f_2'	correction factors in the equation of Grosse and Greffe
M_1, M_2	molar masses
N_A	6.022×10^{23} mol^{-1}
N_1, N_2	number of molecules of each component in 1 cm^3 of the mixture
n_1, n_2	refraction index of the pure components
T	absolute temperature
V_E	excess volume of the mixture
V_m	molar volume of the mixture
V_1, V_2	molar volume of the pure components
x_1	mole fraction of the polar component
x_2	mole fraction of heptane
z_+, z_-	valency of the electrolyte ions
α	polarizability of the mixture
α_1, α_2	polarizability of the pure components
β, β'	interaction parameters of the equation of Heric
γ	reaction field of the polar molecule
ϵ	dielectric constant of the mixture
ϵ_1, ϵ_2	dielectric constant of the pure components
η	dynamic viscosity (in cP) of the mixture
η_1, η_2	dynamic viscosity (in cP) of the pure components
η_1', η_2'	correction factors in the equation of Grosse and Greffe
κ	conductivity (in Ω^{-1} cm^{-1}) of the mixture
κ_1, κ_2	conductivity (in Ω^{-1} cm^{-1}) of the pure components
μ	dipole moment
ν	kinematic viscosity (in cSt) of the mixture
ν_1, ν_2	kinematic viscosity (in cSt) of the pure components
ν_{12}, ν_{21}	binary parameters of the equation of Mc Allister
ρ	density of the mixture
ρ_1, ρ_2	density of the pure components

Literature Cited

(1) Barriol, J., Weisbecker, A., *C.R. Acad. Sci.*, **259**, 2831 (1964).
(2) Böttcher, C. J. F., "Theory of Electric Polarization," 2nd ed, Elsevier, Amsterdam, 1973.
(3) "CRC-Handbook of Chemistry and Physics", 52nd ed, Chemical Rubber Co, Cleveland, Ohio, 1971–1972.
(4) Fuoss, R. M., *J. Am. Chem. Soc.*, **80**, 5059 (1958).
(5) Grosse, C., Greffe, J.-L., *J. Chim. Phys.*, **72**, 1297 (1975).
(6) Heric, E. L., *J. Chem. Eng. Data*, **11**, 66 (1966).
(7) Klinkenberg, A., van der Minne, J. L., "Electrostatics in the Petroleum Industry", Elsevier, Amsterdam, 1958.
(8) Mc Allister, R. A., *AIChE J.*, **6**, 427 (1960).
(9) Onsager, L., *J. Am. Chem. Soc.*, **58**, 1486 (1936).
(10) Rowlinson, J. S., "Liquids and Liquid Mixtures", Butterworths, London, 1959.

Received for review October 12, 1976. Accepted April 1, 1977.

Isopiestic Determination of the Activity Coefficients of Some Aqueous Rare Earth Electrolyte Solutions at 25 °C. 3. The Rare Earth Nitrates

Joseph A. Rard, Loren E. Shiers, David J. Heiser, and Frank H. Spedding*
Ames Laboratory-ERDA and Department of Chemistry, Iowa State University, Ames, Iowa 50011

The osmotic coefficients of the aqueous trinitrates of Sm, Gd, Tb, and Tm have been measured from 0.1–0.2 mol kg^{-1} to saturation, and those of erbium and ytterbium trinitrates have been measured from 0.1 mol kg^{-1} to well into the supersaturated concentration region. In addition, data for La trinitrate have been measured from 0.32 to 1.26 mol kg^{-1}. These osmotic coefficients were fitted to semiempirical least-squares equations, and water activities and mean molal activity coefficients were calculated from these equations. The water activities of these rare earth nitrate solutions are much higher than for the corresponding rare earth chlorides and perchlorates at the same molalities, while the nitrate solution mean molal activity coefficients are much lower. Differences between the activities of the various rare earth salts are discussed in terms of ion–water and ion–ion interactions.

The water activities and activity coefficients of some rare earth chloride (*22*) and perchlorate (*12*) solutions have recently been reported up to saturation at 25 °C. S-Shaped curves result when these properties at constant molality are plotted against the ionic radius of the rare earth ion, from dilute to moderately high concentrations. Although some changes do occur in the shape of these series curves at high concentrations due to the formation of ion-pairs, the shape of each of these series curves over most of the concentration range has been interpreted as being primarily due to changes in the hydration of the rare earth cations. Related series trends also appear in other thermodynamic and transport properties of the rare earth chlorides and perchlorates. The complexes formed in the rare earth chloride and perchlorate solutions are believed to consist predominantly, if not entirely, of outer sphere (i.e., solvent separated) ion-pairs (*2*). Series curves for heats of dilution (*17*), heat capacities (*24*), partial molal volumes (*20*), electrical conductances (*11*), and relative viscosities (*21*) for the rare earth nitrates appear to be S shaped only at relatively low concentrations, while at moderate and high concentrations these properties exhibit more monotone behavior.

Choppin et al. (*2, 3*) have interpreted their spectral and thermodynamic results as indicating that complex formation in dilute rare earth nitrate solutions consists predominantly of outer sphere rare earth nitrate complexes, with a few percent of inner sphere complexes. Ultrasonic absorption results (*5, 15, 16*) suggest that the extent of inner sphere complex formation may be even larger in these solutions. At high concentrations the

amount of inner sphere nitrate complexes formed appears to be quite large (*1, 13*). Three doubly bonded nitrates, and four water molecules, are found to be adjacent to the rare earth ion in the hydrated praseodymium nitrate crystal (*14*). The water activity of a solution is directly related to ionic hydration in that system. Isopiestic measurements were extended to include several of the rare earth nitrates in order to investigate the effect of the formation of rare earth nitrate inner sphere complexes on hydration of the rare earth ion.

Experimental Section

The isopiestic measurements were performed with the same stainless steel isopiestic chambers that were used for the rare earth chloride and perchlorate studies (*12, 22*). Isopiestic equilibrations consist of allowing various solutions to reach thermodynamic equilibrium, through the vapor phase, with a reference solution. All of the equilibrations were performed in sample cups of tantalum metal, using KCl and $CaCl_2$ solutions as the isopiestic reference solutions. Plastic caps were placed on these cups when they were removed from the chambers for weighing. All of the isopiestic measurements were made at 25.00 ± 0.01 °C (IPTS-68). The sample weights were corrected to mass using the rare earth nitrate solution densities of Spedding et al. (*20*), and the KCl and $CaCl_2$ densities were taken from the International Critical Tables. Conductivity water, distilled from an alkaline $KMnO_4$ solution, was used in all solution preparations and dilutions.

The rare earth nitrate solutions were prepared from the rare earth oxides and reagent grade nitric acid. These rare earths had been purified by ion-exchange methods at the Ames Laboratory. The purity of the oxides was greater than 99.85% by weight, with Ca, Fe, Si, and adjacent rare earths being the only significant impurities. The concentration of most of these impurities was below the quantitative detection limit, so the oxides probably were of even greater purity. The stock solutions were adjusted to their equivalence pH values, to ensure a ratio of three nitrates to each rare earth ion (*19*). The dilute samarium and ytterbium nitrate stock solutions, and one of the erbium nitrate stock solutions, that were used for the KCl equilibrations, were analyzed gravimetrically as the oxides. The other rare earth nitrate stock solutions were analyzed by EDTA and gravimetric sulfate methods. The rare earth nitrate samples were evaporated with HCl, before conversion to the sulfates, to destroy the nitrate ions and thereby avoid their coprecipitation. All dilutions for lanthanum, gadolinium, terbium, and thulium nitrates were made from one stock solution, whereas two separately prepared and analyzed stock solutions were used for the other three salts (the Er set 1 dilutions were from the same stock solution as the high concentration Er-$CaCl_2$ equilibrium data). The concentration of each rare earth nitrate stock solution is known to ±0.1% or better in terms of the molality (the exceptions are discussed in the Calculations and Errors section). The preparation and analyses of the KCl and $CaCl_2$ standard solutions are described elsewhere (*22*).

The isopiestic equilibrations for rare earth nitrate solution concentrations above 0.5 mol kg^{-1} were for 4 days to 2 weeks, with the longer times used for the lower concentrations. Equilibration periods of 2–8 weeks were used below 0.5 mol kg^{-1}. Duplicate samples of each rare earth nitrate and reference solution were used, and equilibrium was approached from higher and lower concentrations. The average equilibrium molalities are known to at least ±0.1% above 0.5 mol kg^{-1}, and about ±0.15% at lower concentrations. In many cases the equilibrium molalities were determined more accurately than these limits indicate.

Calculations and Errors

The molal osmotic coefficient of a rare earth nitrate solution is given by

$$\phi = -\frac{1000 \ln a_1}{\nu m M_1} \tag{1}$$

where m is the molal concentration of the solution, M_1 = 18.0154 g mol^{-1} is the molecular weight of water, ν is the number of ions formed when one molecule of solute completely dissociates into its component ions, and a_1 is the activity of water in this solution. If a rare earth nitrate solution is in isopiestic equilibrium with a reference solution, the osmotic coefficient of the rare earth nitrate solution is given by

$$\phi = \frac{\nu^* \phi^* m^*}{\nu m} \tag{2}$$

where the asterisk refers to the reference solution. $CaCl_2$ and KCl were used as isopiestic reference solutions in this study. The osmotic coefficients of $CaCl_2$ were taken from Rard, Habenschuss, and Spedding (*10*), while those of KCl were from Hamer and Wu (*7*) with a small correction applied as described earlier (*9*). The experimental isopiestic molalities and the rare earth nitrate osmotic coefficients are listed in Table I. All concentrations are in terms of the IUPAC-69 atomic weights. Measurements for La nitrate are from 0.32 to 1.26 mol kg^{-1}. The highest concentrations for samarium, gadolinium, terbium, and thulium nitrates are for the saturated solutions. The data for Er extend about 1.7 mol kg^{-1} into the supersaturated region and that for Yb about 1.25 mol kg^{-1}. Four concentrations of Pr nitrate were studied between 0.8 and 1.1 mol kg^{-1}.

The osmotic coefficients for each rare earth nitrate were fitted to least-squares equations of the type

$$\phi = 1 - (A/3)m^{1/2} + \sum_i A_i m^{r_i} \tag{3}$$

where A = (0.510 82)(3)($6^{1/2}$)(2.302 585) = 8.6430. Each osmotic coefficient was given a weight of one or zero for the least-squares fits. The r_i were not constrained to form a consecutive sequence of powers. Substitution of eq 3 into the Gibbs–Duhem relationship and integrating yields

$$\ln \gamma_{\pm} = -Am^{1/2} + \sum_i A_i \left(\frac{r_i + 1}{r_i}\right) m^{r_i} \tag{4}$$

where $\gamma_{\pm}$ is the mean molal activity coefficient of the solute. This equation is the Debye–Hückel limiting law with a series of terms containing powers of the molality. No ion-size term was included in this semiempirical equation since the leading terms of the series alternate in sign and overwhelm any contribution that an ion-size term would make.

The experimental isopiestic data of this research, except for La, extend from about 0.1–0.2 mol kg^{-1} to saturation or supersaturation. Experimental data at lower concentrations are desirable for the extrapolation of the osmotic coefficients to infinite dilution, in order to obtain more precise activity coefficients. No direct experimental activity data are available at lower concentrations for the rare earth nitrate solutions studied in this research except for La. Freezing point depression measurements have been reported for La nitrate (*6*), and heat of dilution (*17*) and heat capacity data (*24*) are available to convert these data to 25 °C.

Heiser (*8*) and Spedding and Jaffe (*18*) have obtained approximate Debye–Hückel ion-size parameters, from dilute solution electrical conductance data, for several of the rare earth nitrates. These å values were used to estimate osmotic coefficients at 0.005, 0.010, 0.015, and 0.020 mol kg^{-1} for samarium, gadolinium, erbium, and ytterbium nitrates from the Debye–Hückel equation. The uncertainty in each of these approximate osmotic coefficients for the rare earth nitrates was estimated to be of the same order as differences across the rare earth series, so averaged values were used at each concentration from 0.005 to 0.020 mol kg^{-1}. When averaged approximate ϕ values for dilute solutions of the rare earth nitrates were used in the

least-squares fits, they connected up smoothly with the isopiestic data for the lighter rare earths (Sm–Tb), and these approximate data were in fair agreement with isopiestic data for the heavier rare earths. These averaged approximate osmotic coefficients for the dilute solutions were included in the least-squares fits to eq 3, except for La, and these values are given in Table I. Freezing point depression data for La (*6*) were converted to osmotic coefficients at 25 °C by standard methods, and these data were used in the least-squares fits along with the isopiestic data. The four lowest concentrations of Hall and Harkins were not included in either Table I or the least-squares fits since these four concentrations and freezing point depressions were determined to only three significant figures.

It was found that seven-term polynomials were adequate to represent the osmotic coefficients of each rare earth nitrate using eq 3. Only five polynomial terms were necessary for La since the data extend over a much smaller concentration range. As for the rare earth chlorides (*22*) and perchlorates (*12*), good fits for the nitrate data were obtained with the three lowest powers fixed at $r_1 = 0.75$, $r_2 = 0.875$, and $r_3 = 1$ while the other four terms were allowed to vary in increments of $m^{1/4}$. The differences between the experimental and calculated ϕ values are given in Table I. The coefficients, powers, and standard deviations for the best fit for each salt are given in Table II. Values of ϕ, a_1, and $\gamma_\pm$ are given in Table III at various selected concentrations.

The $Sm(NO_3)_3$, $Yb(NO_3)_3$, and one set of the $Er(NO_3)_3$ solutions that were used for the KCl equilibrations had been gravimetrically analyzed by conversion to the corresponding rare earth oxides. These gravimetric analyses were performed several years ago (*8*), before it was realized that nitrate ion coprecipitation could be a potential source of error. Nitrate ion coprecipitation would result in high values for the apparent concentrations of the rare earth nitrate stock solutions, giving low values for the osmotic coefficients of their solutions. This can be seen for $Yb(NO_3)_3$ in Figure 1, where the KCl equilibrium data (half-filled circles) are lower than the $CaCl_2$ equilibrium data (filled circles). For $Sm(NO_3)_3$ and $Yb(NO_3)_3$ the error from this source was not very large (about 0.2–0.3%) so the KCl equilibration data for these salts were used in subsequent calculations. The errors in the earlier KCl–$Er(NO_3)_3$ measurements, set 2, were large enough (0.5–0.6% error for ϕ at higher concentrations) that the KCl equilibration data for this salt were redetermined (set 1). Both sets of $Er(NO_3)_3$–KCl data are given in Table I. Many of the $Er(NO_3)_3$ set 2 values were given zero weights in the least-squares fits but the differences between these values and eq 3 are listed to show the size of errors that can occur if nitrate ion coprecipitation occurs during gravimetric analyses.

The errors in the isopiestic data due to stock solution concentration errors, and uncertainties in the equilibration molalities, have been discussed in detail elsewhere (*22*). The total expected errors for ϕ, relative to the reference solution ϕ values, are about 0.3% above 0.5 mol kg^{-1} and 0.34% below this concentration, with the probable errors being about two-thirds of these values. The errors for the osmotic coefficients of the isopiestic reference solutions also need to be considered in determining the absolute errors for the data (*10*). Since it was necessary to estimate activity data below 0.1 mol kg^{-1} for six of the salts, the activity coefficients of the rare earth nitrates could have absolute errors as large as 1–2%. Relative errors in these properties as a function of concentration, for each salt, will be much smaller than the above error limits indicate.

The standard deviations of eq 3 ranged from 0.0006 to 0.0017 for the various rare earth nitrates, which, in most cases, is smaller than the standard deviation for the corresponding rare earth chloride (*22*). The differences between the experimental and calculated osmotic coefficients of $Yb(NO_3)_3$ are illustrated in Figure 1, and nearly all of the experimental data fall within ±0.2% of eq 3.

The osmotic coefficients of the rare earth chlorides (*22*), perchlorates (*12*), and nitrates were fitted to series with seven powers in $m^{1/8}$, and these powers were not required to be consecutive. Nine parameter series in $m^{1/2}$ with sequential powers also worked about as well as the fits finally picked, for most of these salts, while seven term sequential series in $m^{1/2}$ had standard deviations about three to four times larger than the best fits. For a few salts, such as $Yb(NO_3)_3$, nine terms in $m^{1/2}$ did not do nearly as well as the $m^{1/8}$ fits. If integral powers in m were used rather than half integral powers, then the resulting fits gave a much poorer representation of the experimental data. We chose the $m^{1/8}$ series in preference to the $m^{1/2}$ series since two fewer terms were required, and the $m^{1/8}$ series worked for all of the salts.

The molal solubilities of the nitrates of Sm, Gd, Tb, and Tm were determined by the isopiestic method, and these solubilities are listed as the highest concentration, for each of these salts, in Table I. These concentrations differ from direct analyses values (*11*) by 0.07–0.17%, and this is well within the combined uncertainties of these two determinations.

Results

Figures 2–4 are plots of ln $\gamma_\pm$, ϕ, and a_1 for $Yb(ClO_4)_3$, $YbCl_3$, and $Yb(NO_3)_3$. It can be seen that no distinct changes occur when supersaturated concentrations are reached (above 6.65 mol kg^{-1} for $Yb(NO_3)_3$). The values of ln $\gamma_\pm$ and ϕ for $Yb(ClO_4)_3$ are appreciably higher than the values for $YbCl_3$, while those of $Yb(NO_3)_3$ are much lower than for $YbCl_3$. The $Yb(NO_3)_3$ water activities are highest and the $Yb(ClO_4)_3$ values lowest.

In the rare earth perchlorate activity paper (*12*) it was noted that differences in anion–water interactions are required to explain differences between the rare earth chloride and perchlorate data, and that the perchlorate ion appears to be more extensively hydrated than the chloride ion. The symmetry of the uncomplexed nitrate ion in aqueous solution is known to be reduced from the expected D_{3h} symmetry, and this reduction in symmetry has been interpreted in terms of the formation of one fairly strong hydrogen bond between the nitrate ion and a water molecule (*4*). The rare earth nitrates form appreciable amounts of inner sphere complexes (*1–3, 5, 13, 15, 16*), especially at high concentrations. The formation of inner sphere complexes will result in the displacement of water from the rare earth ion's inner sphere, and will reduce the charge on the rare earth ion. Consequently, inner sphere complex formation is probably much more important than nitrate ion–water interactions in determining the thermodynamic properties of rare earth nitrate solutions. The water activities of the rare earth nitrate solutions are not as low as for the chlorides and perchlorates (Figure 4), mainly due to the release of inner sphere water as inner sphere complex formation occurs in the nitrate solutions. This factor, together with the reduction in the charge and number of ions in these solutions, accounts for the fact that the rare earth nitrate ln $\gamma_\pm$ values are not as high as the chloride and perchlorate values. This displacement of rare earth ion inner sphere water by the nitrate ion is also observed in ultrasonic absorption experiments (*15, 16*). If a rare earth nitrate solution is diluted, the amount of outer sphere complexes should increase relative to the amount of inner sphere complexes. This can be seen to occur in Figures 2–4 where, at relatively low concentrations, the nitrate curves approach the chloride curves.

Plots of $\gamma_\pm$, ϕ, and a_1, at various constant molalities, are shown as a function of the ionic radius (*23*) in Figures 5–7. Comparison of the nitrate solution series trends with the series trends for the chlorides and perchlorates indicates that the osmotic and activity coefficients for $La(NO_3)_3$ are slightly higher than expected, below 0.6 mol kg^{-1}, while the water activities are slightly lower. Above 0.6 mol kg^{-1}, the shapes of these rare earth nitrate series curves change from the trends found at 0.4 mol kg^{-1}, with a_1 decreasing regularly from La to Yb, and ϕ and

Table I. Isopiestic Molalities and Osmotic Coefficients of Some Rare Earth Nitrates

m, $Re(NO_3)_3$	m, standard	ϕ, $Re(NO_3)_3$	$10^3\Delta\phi$
	$La(NO_3)_3$, freezing point depression		
0.022 311	—	0.7935	−0.5
0.023 699	—	0.7898	−1.5
0.043 599	—	0.7685	1.2
0.051 483	—	0.7629	1.0
0.087 282	—	0.7509	1.6
0.177 14	—	0.7438	−3.3
	$La(NO_3)_3$ vs. KCl		
0.316 85	0.537 97	0.7629	0.9
0.361 94	0.619 39	0.7681	0.1
0.408 02	0.703 27	0.7731	−1.3
0.429 69	0.746 99	0.7796	2.0
0.808 62	1.496 8	0.8354	0.0
1.013 0	1.930 9	0.8673	−0.6
1.122 6	2.172 6	0.8853	−0.1
1.261 9	2.485 8	0.9081	0.4
	$Pr(NO_3)_3$ vs. KCl		
0.804 67	1.496 8	0.8395	—
0.904 50	1.712 9	0.8579	—
1.002 0	1.930 9	0.8768	—
1.108 4	2.172 6	0.8967	—
	$Sm(NO_3)_3$ (from conductance)		
0.005 00	—	0.8606	0.8
0.010 00	—	0.8277	−0.3
0.015 00	—	0.8084	−0.7
0.020 00	—	0.7952	−0.8
	$Sm(NO_3)_3$ vs. KCl		
0.105 35	0.171 29	0.7441	2.4
0.126 98	0.206 77	0.7424	2.7
0.187 39	0.304 27	0.7351	−4.8
0.345 84	0.582 86	0.7567	−0.9
0.381 55	0.648 08	0.7621	−1.1
0.442 86	0.765 30	0.7749	1.1
0.519 18	0.914 12	0.7896	1.4
0.731 44	1.353 2	0.8331	−0.1
0.857 01	1.634 2	0.8626	0.3
0.895 92	1.725 0	0.8724	0.9
0.905 66	1.747 7	0.8748	0.9
0.937 58	1.821 4	0.8819	0.3
1.028 5	2.039 2	0.9042	0.4
1.238 7	2.558 4	0.9539	−2.7
1.363 3	2.881 3	0.9848	−3.7
1.523 0	3.317 9	1.0281	−1.5
	$Sm(NO_3)_3$ vs. $CaCl_2$		
1.216 8	1.345 6	0.9521	1.1
1.278 2	1.409 5	0.9666	−0.1
1.339 5	1.474 5	0.9826	0.3
1.400 1	1.537 2	0.9974	−0.5
1.461 9	1.603 6	1.0152	1.3
1.541 6	1.687 3	1.0367	2.3
1.636 1	1.782 0	1.0590	0.2
1.718 7	1.866 5	1.0807	0.6
1.814 8	1.962 7	1.1047	−0.1
1.914 6	2.062 6	1.1303	0.1
2.006 6	2.153 2	1.1533	−0.3
2.103 4	2.248 5	1.1780	0.0
2.199 0	2.341 1	1.2017	−0.2
2.278 1	2.418 1	1.2219	0.4
2.399 5	2.533 6	1.2514	0.1
2.491 5	2.620 5	1.2737	0.2
2.588 9	2.711 4	1.2968	0.0
2.690 8	2.806 2	1.3212	0.2
2.792 5	2.899 6	1.3449	0.2
2.910 0	3.006 1	1.3716	−0.1
3.014 3	3.099 7	1.3949	−0.3
3.126 7	3.200 9	1.4206	0.3
3.219 4	3.282 7	1.4407	0.2
3.331 9	3.380 3	1.4642	−0.7
3.444 1	3.478 7	1.4886	−0.1
3.538 0	3.560 4	1.5087	0.4
3.634 4	3.642 3	1.5280	−0.2
3.731 5	3.725 6	1.5481	0.1
3.845 6	3.822 3	1.5710	0.1
3.935 9	3.897 4	1.5881	−0.6
4.040 8	3.986 4	1.6094	0.1
4.139 6	4.068 9	1.6285	0.1
4.213 8	4.130 9	1.6428	0.3
4.257 7	4.166 7	1.6507	−0.2
4.277 4	4.183 4	1.6547	0.0
	$Gd(NO_3)_3$ (from conductance)		
0.005 00	—	0.8606	0.0
0.010 00	—	0.8277	0.0
0.015 00	—	0.8084	0.0
0.020 00	—	0.7952	0.0
	$Gd(NO_3)_3$ vs. KCl		
0.210 74	0.353 76	0.7581	−0.1
0.583 08	1.075 6	0.8281	−0.9
0.641 90	1.203 0	0.8424	0.3
0.775 73	1.500 9	0.8732	0.1
0.876 46	1.736 8	0.8981	0.4
1.016 6	2.077 4	0.9328	−0.3
1.136 4	2.384 0	0.9646	0.2
1.221 8	2.609 2	0.9877	0.5
1.366 2	2.999 6	1.0265	0.2
1.429 4	3.168 8	1.0415	−2.1
	$Gd(NO_3)_3$ vs. $CaCl_2$		
0.358 52	0.417 48	0.7841	1.0
0.413 88	0.480 28	0.7929	−0.8
1.158 5	1.317 0	0.9710	0.7
1.757 3	1.956 5	1.1353	0.5
2.005 3	2.231 2	1.2206[a]	16.6
2.160 6	2.369 6	1.2470	0.0
2.421 6	2.629 9	1.3182	0.0
2.485 0	2.692 3	1.3353	0.0
2.492 3	2.699 9	1.3376	0.3
2.516 5	2.723 1	1.3437	−0.1
2.575 1	2.781 4	1.3602	0.8
2.584 2	2.788 8	1.3615	−0.4
2.600 0	2.804 4	1.3659	−0.2
2.621 2	2.825 1	1.3716	−0.1
2.739 9	2.939 6	1.4027	−0.1
2.763 5	2.962 5	1.4090	0.1
2.804 0	3.001 5	1.4197	0.3
2.805 5	3.003 2	1.4203	0.5
2.872 4	3.065 7	1.4366	−0.5
2.920 4	3.111 8	1.4493	−0.1
3.028 8	3.213 6	1.4765	−0.3
3.048 9	3.232 4	1.4815	−0.3
3.126 4	3.305 1	1.5010	−0.1
3.199 0	3.373 1	1.5194	0.4
3.368 6	3.528 2	1.5597	−0.4
3.418 8	3.574 2	1.5718	−0.2
3.483 6	3.634 0	1.5878	0.5
3.594 8	3.734 1	1.6134	0.1
3.708 2	3.836 1	1.6395	0.3
4.032 4	4.123 9	1.7116	0.6
4.101 6	4.181 9	1.7245	−1.5
4.229 3	4.296 4	1.7536	0.5
4.370 1	4.418 5	1.7825	0.1
	$Tb(NO_3)_3$ (from conductance)		
0.005 00	—	0.8606	0.8
0.010 00	—	0.8277	0.3
0.015 00	—	0.8084	−0.3
0.020 00	—	0.7952	−0.9
	$Tb(NO_3)_3$ vs. KCl		
0.206 66	0.353 76	0.7731	1.1

Table I (continued)

m, $Re(NO_3)_3$	m, standard	ϕ, $Re(NO_3)_3$	$10^3\Delta\phi$	m, $Re(NO_3)_3$	m, standard	ϕ, $Re(NO_3)_3$	$10^3\Delta\phi$
0.568 90	1.075 6	0.8487	−1.7		$Er(NO_3)_3$ vs. KCl, set 2		
0.626 39	1.203 0	0.8632	−0.8	0.105 03	0.182 24	0.7931[a]	12.4
0.756 84	1.500 9	0.8950	−0.6	0.159 90	0.279 12	0.7914	1.7
0.855 30	1.736 8	0.9203	0.0	0.184 31	0.325 83	0.7994	4.6
0.992 71	2.077 4	0.9552	−0.3	0.294 14	0.535 92	0.8187	−2.6
1.111 0	2.384 0	0.9867	0.1	0.300 83	0.551 37	0.8233	0.3
1.194 6	2.609 2	1.0102	1.3	0.455 18	0.883 98	0.8709[a]	5.3
1.338 0	2.999 6	1.0481	0.6	0.567 78	1.130 5	0.8943[a]	−4.4
1.399 8	3.168 8	1.0636	−0.8	0.634 85	1.289 8	0.9141[a]	−4.9
				0.705 08	1.463 0	0.9359[a]	−4.7
	$Tb(NO_3)_3$ vs. $CaCl_2$			0.891 75	1.943 8	0.9920[a]	−6.8
0.350 59	0.417 48	0.8019	0.6	1.012 8	2.273 5	1.0294[a]	−7.6
0.404 42	0.480 28	0.8115	−1.6	1.184 7	2.765 5	1.0842[a]	−6.7
0.660 14	0.783 35	0.8753	3.2	1.268 6	3.009 5	1.1094[a]	−7.7
1.134 0	1.317 0	0.9919	−0.7	1.363 2	3.294 3	1.1396[a]	−6.7
1.569 6	1.789 9	1.1112	0.4	1.407 4	3.429 8	1.1539[a]	−6.0
1.728 5	1.956 5	1.1542	−0.3	1.495 0	3.688 7	1.1777[a]	−8.9
1.746 4	1.976 2	1.1601	0.6	1.539 0	3.824 0	1.1910[a]	−8.9
1.994 2	2.231 2	1.2274	−0.2	1.687 8	4.292 6	1.2376[a]	−6.7
2.131 2	2.369 6	1.2642	−0.8	1.750 2	4.484 7	1.2547[a]	−8.0
2.154 6	2.394 6	1.2718	0.4		$Er(NO_3)_3$ vs. $CaCl_2$		
2.279 6	2.519 1	1.3050	−0.2	0.972 85	1.203 5	1.0236	−0.8
2.391 4	2.629 9	1.3349	−0.3	1.035 4	1.278 1	1.0429	−1.2
2.454 8	2.692 3	1.3518	−0.3	1.146 3	1.409 5	1.0778	−1.1
2.465 6	2.703 4	1.3550	0.1	1.201 5	1.474 5	1.0955	−0.7
2.485 2	2.723 1	1.3606	0.5	1.255 9	1.537 2	1.1119	−1.2
2.553 9	2.788 8	1.3776	−0.7	1.312 5	1.603 6	1.1307	0.0
2.569 6	2.804 4	1.3820	−0.4	1.384 7	1.687 3	1.1542	1.3
2.733 4	2.962 5	1.4245	−0.7	1.469 9	1.782 0	1.1788	−0.2
2.794 2	3.022 1	1.4413	0.4	1.545 1	1.866 5	1.2021	0.4
2.961 8	3.180 4	1.4833	−0.4	1.632 9	1.962 7	1.2277	−3.0
3.016 6	3.232 4	1.4973	−0.1	1.724 4	2.062 6	1.2550	−0.1
3.044 1	3.259 0	1.5048	0.5	1.808 9	2.153 2	1.2793	−0.4
3.186 4	3.391 4	1.5397	0.1	1.898 3	2.248 5	1.3053	−0.2
3.223 2	3.425 9	1.5490	0.4	1.986 5	2.341 1	1.3302	−0.3
3.305 6	3.501 8	1.5688	0.2	2.060 0	2.418 1	1.3513	0.2
3.471 0	3.655 2	1.6098	1.5	2.172 6	2.533 6	1.3821	−0.1
3.505 4	3.684 2	1.6161	−0.3	2.258 0	2.620 5	1.4054	0.1
3.617 3	3.785 4	1.6420	−0.5	2.272 6	2.634 1	1.4084	−0.9
3.631 6	3.799 8	1.6465	0.6	2.349 0	2.711 4	1.4293	−0.4
3.770 8	3.923 6	1.6773	−0.5	2.412 9	2.774 8	1.4459	−0.6
3.803 2	3.953 5	1.6853	0.1	2.444 0	2.806 2	1.4546	0.0
3.934 4	4.069 3	1.7137	−0.8	2.538 4	2.899 6	1.4795	0.4
4.041 0	4.164 5	1.7376	−0.3	2.600 4	2.958 1	1.4937	−1.2
4.141 2	4.254 1	1.7601	0.5	2.648 4	3.006 1	1.5070	0.1
4.189 0	4.293 1	1.7681	−1.8	2.745 9	3.099 7	1.5312	−0.1
4.211 0	4.316 8	1.7759	1.4	2.825 5	3.174 6	1.5500	−0.9
4.332 4	4.420 5	1.7994	−0.7	2.850 9	3.200 9	1.5580	0.9
4.460 4	4.534 1	1.8271	0.6	2.938 5	3.282 7	1.5784	0.2
4.466 0	4.537 3	1.8270	−0.6	2.986 9	3.326 3	1.5885	−1.2
4.532 0	4.596 8	1.8418	0.8	3.043 3	3.380 3	1.6030	−0.1
				3.149 0	3.478 7	1.6281	0.3
	$Er(NO_3)_3$ (from conductance)			3.237 8	3.560 4	1.6485	0.4
0.005 00	—	0.8606	5.7	3.241 6	3.561 3	1.6473	−1.7
0.010 00	—	0.8277	1.0	3.327 2	3.642 3	1.6690	0.6
0.015 00	—	0.8084	−3.0	3.409 8	3.715 2	1.6859	−0.9
0.020 00	—	0.7952	−6.5	3.418 9	3.725 6	1.6896	0.8
				3.526 9	3.822 3	1.7129	0.4
	$Er(NO_3)_3$ vs. KCl, set 1			3.610 2	3.897 4	1.7314	0.9
0.100 40	0.172 06	0.7842	4.1	3.627 4	3.910 5	1.7334	−0.9
0.104 28	0.178 14	0.7812	0.6	3.710 9	3.986 4	1.7525	0.4
0.295 28	0.537 97	0.8186	−3.0	3.803 8	4.068 9	1.7722	0.7
0.335 26	0.619 39	0.8292	−2.9	3.844 1	4.102 2	1.7789	−1.0
0.375 56	0.703 27	0.8399	−3.2	3.873 8	4.130 9	1.7870	0.9
0.394 79	0.746 99	0.8485	0.1	3.914 3	4.166 7	1.7955	1.1
0.714 71	1.496 8	0.9451	1.6	3.928 9	4.178 0	1.7973	−0.1
0.798 28	1.712 9	0.9720	2.5	3.931 5	4.180 6	1.7981	0.2
0.880 77	1.930 9	0.9975	2.1	3.935 7	4.185 2	1.7997	0.9
0.969 84	2.172 6	1.0248	1.4	3.989 2	4.232 4	1.8108	1.1
1.082 1	2.485 8	1.0590	0.3	4.019 8	4.255 8	1.8145	−1.4
1.216 5	2.877 2	1.1019	1.1				

Table I (continued)

m, $Re(NO_3)_3$	m, standard	ϕ, $Re(NO_3)_3$	$10^3\Delta\phi$
4.103 7	4.333 7	1.8348	2.1
4.196 8	4.412 3	1.8515	0.3
4.247 8	4.457 3	1.8621	0.8
4.283 4	4.487 8	1.8687	0.5
4.410 9	4.598 7	1.8937	0.9
4.479 7	4.655 4	1.9048	−1.1
4.498 9	4.674 2	1.9100	0.5
4.632 3	4.789 2	1.9349	0.4
4.669 4	4.816 4	1.9384	−3.0
4.722 3	4.867 0	1.9515	0.4
4.791 0	4.926 5	1.9642	0.6
4.865 5	4.991 4	1.9780	0.9
4.889 8	5.008 4	1.9796	−1.8
4.957 4	5.070 7	1.9943	0.8
5.079 4	5.176 4	2.0156	0.7
5.139 1	5.222 5	2.0222	−3.0
5.237 9	5.314 8	2.0432	1.0
5.307 7	5.373 9	2.0538	−0.2
5.358 1	5.417 5	2.0619	−0.6
5.457 2	5.507 2	2.0799	0.9
5.523 3	5.561 1	2.0880	−1.8
5.533 3	5.570 3	2.0898	−1.6
5.539 7	5.581 5	2.0943	1.7
5.549 0	5.582 6	2.0914	−2.6
5.643 7	5.667 7	2.1072	−2.1
5.650 5	5.679 8	2.1119	1.5
5.747 2	5.760 9	2.1240	−1.8
5.747 7	5.766 6	2.1271	1.2
5.816 7	5.828 5	2.1377	1.0
5.836 6	5.842 2	2.1383	−1.5
5.882 0	5.886 5	2.1471	0.2
5.945 2	5.945 6	2.1575	1.0
5.946 5	5.943 8	2.1560	−0.7
5.980 1	5.981 4	2.1649	3.1
5.980 9	5.978 5	2.1630	1.0
6.026 6	6.022 0	2.1707	1.8
6.053 9	6.041 6	2.1717	−1.4
6.176 6	6.156 3	2.1900	−1.2
6.192 0	6.178 4	2.1963	2.8
6.268 3	6.242 6	2.2032	−1.4
6.400 3	6.369 0	2.2219	−1.4
6.510 9	6.482 8	2.2403	1.6
6.625 4	6.592 6	2.2540	−0.2
6.696 9	6.666 2	2.2643	0.6
6.769 7	6.737 5	2.2726	−0.6
6.852 1	6.824 6	2.2842	0.4
6.921 0	6.895 6	2.2925	0.0
6.990 1	6.969 2	2.3014	0.4
7.089 2	7.071 7	2.3119	−1.0
7.167 9	7.160 6	2.3226	0.4
7.270 9	7.272 0	2.3337	−0.3
	$Tm(NO_3)_3$ (from conductance)		
0.005 00	—	0.8606	3.2
0.010 00	—	0.8277	1.1
0.015 00	—	0.8084	−1.0
0.020 00	—	0.7952	−3.2
	$Tm(NO_3)_3$ vs. KCl		
0.199 96	0.353 76	0.7990	1.4
0.538 30	1.075 6	0.8970	−1.1
0.591 31	1.203 0	0.9144	−0.6
0.710 34	1.500 9	0.9536	−0.1
0.800 42	1.736 8	0.9834	−0.2
0.925 28	2.077 4	1.0248	−0.6
1.108 8	2.609 2	1.0883	1.0
1.239 4	2.999 6	1.1315	0.1
1.295 6	3.168 8	1.1491	−1.1
	$Tm(NO_3)_3$ vs. $CaCl_2$		
0.335 69	0.417 48	0.8375	1.4
0.385 90	0.480 28	0.8504	−0.6
1.052 8	1.317 0	1.0684	0.0
1.452 4	1.789 9	1.2009	−1.3
1.595 2	1.956 5	1.2507	2.0
1.615 4	1.976 2	1.2541	−1.0
1.739 8	2.115 3	1.2937	−1.0
1.841 2	2.231 2	1.3294	3.0
1.969 2	2.369 6	1.3682	2.8
1.996 2	2.394 6	1.3727	−0.8
2.113 6	2.519 1	1.4075	−0.8
2.274 7	2.692 3	1.4588	4.2
2.290 8	2.703 4	1.4584	−0.7
2.391 2	2.804 4	1.4851	−2.0
2.494 8	2.910 0	1.5144	−0.8
2.607 8	3.022 1	1.5443	−0.9
2.769 8	3.180 4	1.5861	−0.8
2.851 4	3.259 0	1.6065	−0.8
2.990 2	3.391 4	1.6407	−0.4
3.026 8	3.425 9	1.6495	−0.4
3.108 7	3.501 8	1.6682	−1.0
3.273 4	3.655 2	1.7069	−0.1
3.431 3	3.799 8	1.7426	0.5
3.603 4	3.953 5	1.7787	−0.3
3.680 7	4.022 2	1.7948	−0.4
3.799 0	4.127 0	1.8192	−0.2
3.926 2	4.239 2	1.8451	0.2
3.990 8	4.296 0	1.8581	0.6
4.053 1	4.350 2	1.8702	0.5
4.174 6	4.455 2	1.8932	0.3
4.244 6	4.516 5	1.9069	0.9
4.381 4	4.632 8	1.9311	−0.1
4.541 1	4.770 5	1.9604	0.4
4.735 8	4.937 8	1.9949	0.8
4.811 4	5.001 7	2.0073	0.3
4.885 6	5.066 8	2.0209	1.3
4.958 1	5.128 2	2.0325	0.8
5.077 0	5.228 1	2.0507	−0.6
5.112 6	5.259 0	2.0566	−0.4
5.161 8	5.300 6	2.0641	−0.9
5.204 0	5.337 6	2.0713	−0.5
5.359 7	5.471 7	2.0954	−0.9
5.532 5	5.623 1	2.1224	−0.4
5.578 0	5.662 5	2.1289	−0.7
5.737 3	5.803 5	2.1526	−0.5
5.792 2	5.850 3	2.1594	−1.7
5.952 6	6.002 0	2.1865	2.8
	$Yb(NO_3)_3$ (from conductance)		
0.005 00	—	0.8606	4.7
0.010 00	—	0.8277	1.4
0.015 00	—	0.8084	−1.7
0.020 00	—	0.7952	−4.6
	$Yb(NO_3)_3$ vs. KCl		
0.096 766	0.166 56	0.7882[a]	9.7
0.116 94	0.204 54	0.7976[a]	16.0
0.171 97	0.300 87	0.7922	−1.1
0.187 35	0.331 82	0.8007	3.7
0.190 55	0.337 34	0.8001	2.3
0.281 76	0.513 59	0.8194	−2.5
0.414 78	0.795 42	0.8599	−0.8
0.477 74	0.937 86	0.8805	0.2
0.542 54	1.086 9	0.8994	−1.6
0.583 44	1.185 9	0.9134	−1.0
0.709 30	1.506 9	0.9589	1.9
0.757 48	1.633 8	0.9756	2.0
0.873 02	1.943 8	1.0133	−1.0
0.989 05	2.273 5	1.0541	−1.6
1.114 8	2.646 4	1.0990	−1.9
1.189 2	2.872 2	1.1251	−2.6
1.322 5	3.294 3	1.1747	−0.7
1.365 8	3.429 8	1.1891	−1.7
1.501 7	3.867 9	1.2364	−2.4
1.630 2	4.292 6	1.2813	−2.0

[a] Extrapolated.

Table I (continued)

m, $Re(NO_3)_3$	m, standard	ϕ, $Re(NO_3)_3$	$10^3\Delta\phi$	m, $Re(NO_3)_3$	m, standard	ϕ, $Re(NO_3)_3$	$10^3\Delta\phi$
1.687 0	4.484 7	1.3017	−1.0	4.043 3	4.412 3	1.9218	−0.4
	$Yb(NO_3)_3$ vs. $CaCl_2$			4.128 5	4.487 8	1.9389	0.4
1.067 5	1.345 6	1.0853	1.4	4.256 6	4.598 7	1.9624	0.0
1.119 8	1.409 5	1.1033	0.6	4.345 0	4.674 2	1.9777	−0.7
1.172 5	1.474 5	1.1226	0.9	4.477 6	4.789 2	2.0017	−0.2
1.224 5	1.537 2	1.1405	0.1	4.567 6	4.867 0	2.0176	0.2
1.277 8	1.603 6	1.1614	2.0	4.638 5	4.926 5	2.0288	−0.7
1.346 4	1.687 3	1.1871	3.2	4.713 1	4.991 4	2.0420	0.0
1.427 9	1.782 0	1.2134	0.7	4.807 0	5.070 7	2.0566	−0.7
1.499 1	1.866 5	1.2390	1.2	4.929 1	5.176 4	2.0771	0.1
1.581 9	1.962 7	1.2673	0.7	5.090 9	5.314 8	2.1022	0.1
1.668 2	2.062 6	1.2973	1.0	5.212 2	5.417 5	2.1196	−0.9
1.748 5	2.153 2	1.3235	0.0	5.316 4	5.507 2	2.1350	−0.9
1.832 5	2.248 5	1.3521	0.5	5.400 9	5.581 5	2.1481	−0.1
1.915 9	2.341 1	1.3792	0.1	5.512 5	5.679 8	2.1648	0.8
1.985 3	2.418 1	1.4021	0.6	5.612 3	5.766 6	2.1784	0.5
2.091 4	2.533 6	1.4358	0.5	5.684 0	5.828 5	2.1876	−0.1
2.172 3	2.620 5	1.4609	0.3	5.749 3	5.886 5	2.1966	0.1
2.258 1	2.711 4	1.4868	0.0	5.815 8	5.945 6	2.2055	0.1
2.348 4	2.806 2	1.5138	0.0	5.853 3	5.978 5	2.2102	−0.2
2.437 7	2.899 6	1.5406	0.6	5.855 3	5.981 4	2.2111	0.5
2.542 4	3.006 1	1.5699	−0.1	5.900 0	6.022 0	2.2173	0.8
2.635 8	3.099 7	1.5952	−0.9	6.071 0	6.178 4	2.2401	1.8
2.735 7	3.200 9	1.6236	0.3	6.202 7	6.296 3	2.2547	0.1
2.818 8	3.282 7	1.6455	0.0	6.321 2	6.406 2	2.2687	−0.2
2.919 1	3.380 3	1.6712	−0.3	6.446 0	6.525 4	2.2838	0.3
3.020 8	3.478 7	1.6972	−0.2	6.560 8	6.637 1	2.2975	0.8
3.106 1	3.560 4	1.7184	0.0	6.658 1	6.729 7	2.3071	−0.4
3.193 2	3.642 3	1.7391	−0.4	6.752 1	6.823 6	2.3176	−0.1
3.282 0	3.725 6	1.7601	−0.4	6.849 0	6.921 0	2.3277	−0.1
3.385 6	3.822 3	1.7844	0.1	6.965 6	7.042 2	2.3405	0.7
3.466 0	3.897 4	1.8035	1.0	7.082 0	7.163 1	2.3518	0.5
3.562 3	3.986 4	1.8256	1.9	7.203 1	7.286 2	2.3612	−1.7
3.655 7	4.068 9	1.8440	0.3	7.321 3	7.415 8	2.3729	−0.9
3.725 3	4.130 9	1.8582	−0.1	7.414 5	7.518 2	2.3813	−0.7
3.765 2	4.166 7	1.8666	−0.1	7.523 5	7.637 1	2.3899	−1.3
3.778 6	4.178 0	1.8688	−0.6	7.620 3	7.745 1	2.3977	−1.4
3.781 8	4.180 6	1.8693	−0.8	7.725 3	7.869 4	2.4079	0.8
3.785 6	4.185 2	1.8710	0.2	7.837 9	7.997 4	2.4163	1.0
3.839 1	4.232 4	1.8816	−0.2	7.911 5	8.082 1	2.4218	1.4
3.953 4	4.333 7	1.9046	0.0				

[a] This point given a weight of zero in the least-squares fit.

ln $\gamma_\pm$ increasing from La to Yb (the La data extend only to 1.26 mol kg^{-1}). Additional data for rare earth nitrates will be required, especially for La at higher concentrations and for Ce, Pr, and Nd at all concentrations, before anything more definite can be concluded about series trends for these properties.

The a_1 series curves for the rare earth chlorides and perchlorates (*12, 22*) are S shaped from dilute solution to over 2.0 mol kg^{-1}. At higher concentrations the water activities separate into two series with the Sm to Lu data displaced from the La to Nd data. The S shape at low concentrations was attributed to the effect of the decreasing ionic radius of the rare earth ion as the lanthanide contraction occurs. The smaller ions should have larger surface charge densities, and thereby affect more water molecules, than the rare earths with the larger radii. This accounts for the decrease in a_1 from La to Nd–Sm and from Tb–Dy to Lu. Superimposed on this is an inner sphere hydration number decrease that begins to occur after a critical size is reached at Nd (*19*). This hydration number decrease is believed to be complete by Tb. The loss of one inner sphere water should reduce the shielding of the second row and more distant water molecules from the rare earth ion's electrical charge, by the first-row waters, and also cause the radius of the rare earth ions' inner hydration sphere to decrease. X-ray diffraction experiments, now in progress at this laboratory, indicate that the rare earth ion–inner sphere water distance does decrease as the atomic number of the rare earth ion increases. The net result of the rare earth inner sphere hydration number change is to cause total cation hydration to increase more rapidly with decreasing ionic radius, as increasing numbers of second row and more distant waters are affected between Nd and Tb, giving rise to the S-shaped series curves. At higher concentrations ion-pairing effects appear to become quite large, and some modifications of the series trends do occur. However, the inner sphere hydration number decrease still probably occurs in the rare earth chlorides and perchlorates at high concentrations.

This same mechanism should apply to very dilute solutions of the rare earth nitrates, and break down when significant amounts of rare earth nitrate inner sphere complexes are formed. Electrical conductance data for the rare earth nitrate solutions (*11*) indicate that the amount of complex formation increases from La to Sm–Eu, and then decreases to Lu, from a few millimolal up to 0.8–0.9 mol kg^{-1}. At higher concentrations the amount of complex formation decreases from La to Yb–Lu at constant molality. Since at least part of this complex formation involves the displacement of inner sphere water held by the rare earth ion, the activity data for these solutions might be expected

Table II. Coefficients and Powers for Osmotic Coefficient Polynomials

i	r_i	A_i	r_i	A_i
		$La(NO_3)_3$		$Sm(NO_3)_3$
1	0.75	−10.537 645	0.75	−18.288 175
2	0.875	53.708 079	0.875	85.679 632
3	1	−56.010 500	1	−95.058 396
4	1.25	19.442 742	1.25	42.688 874
5	1.5	−3.855 881 4	1.5	−14.227 937
6.	—	—	1.75	1.983 729 2
7	—	—	4.5	$5.522\ 533\ 6 \times 10^{-5}$
S.D.		0.001 7		0.001 3
		$Gd(NO_3)_3$		$Tb(NO_3)_3$
1	0.75	−5.699 954 0	0.75	−8.618 894 0
2	0.875	25.973 154	0.875	39.828 968
3	1	−11.454 991	1	−32.295 273
4	1.25	−24.576 207	1.75	12.364 466
5	1.5	31.022 616	2	−12.151 824
6	1.75	−15.185 822	2.25	3.858 813 7
7	2	2.730 999 1	2.75	−0.147 873 4
S.D.		0.000 6		0.000 9
		$Er(NO_3)_3$		$Tm(NO_3)_3$
1	0.75	−30.452 134	0.75	−12.842 720
2	0.875	129.527 29	0.875	53.484 047
3	1	−138.102 73	1	−43.468 579
4	1.25	50.325 413	1.75	19.973 736
5	1.75	−13.339 390	2	−21.050 763
6	2	5.181 235 3	2.25	7.141 753 1
7	2.5	−0.225 780 71	2.75	−0.305 870 3
S.D.		0.001 6		0.001 4
		$Yb(NO_3)_3$		
1	0.75	−18.320 061		
2	0.875	74.073 538		
3	1	−64.015 223		
4	1.5	17.697 417		
5	2	−12.561 611		
6	2.25	7.396 263 5		
7	2.5	−1.329 717 6		
S.D.		0.001 3		

Table III. Osmotic Coefficients, Water Activities, and Activity Coefficients at Even Molalities

m	ϕ	a_1	$\gamma_\pm$	m	ϕ	a_1	$\gamma_\pm$
		$La(NO_3)_3$		1.4	0.9979	0.904 23	0.2217
0.1	0.7475	0.994 628	0.3025	1.6	1.0495	0.886 0	0.2341
0.2	0.7489	0.989 27	0.2541	1.8	1.1009	0.866 9	0.2487
0.3	0.7598	0.983 71	0.2325	2.0	1.1519	0.847 0	0.2652
0.4	0.7733	0.977 96	0.2203	2.2	1.2021	0.826 5	0.2836
0.5	0.7878	0.972 01	0.2129	2.4	1.2514	0.805 4	0.3038
0.6	0.8029	0.965 88	0.2082	2.6	1.2995	0.783 9	0.3259
0.7	0.8183	0.959 56	0.2053	2.8	1.3464	0.762 1	0.3498
0.8	0.8340	0.953 06	0.2038	3.0	1.3920	0.740 1	0.3756
0.9	0.8498	0.946 37	0.2032	3.2	1.4363	0.718 1	0.4032
1.0	0.8658	0.939 52	0.2034	3.4	1.4793	0.696 0	0.4328
1.2	0.8978	0.925 30	0.2055	3.6	1.5211	0.673 9	0.4643
1.2619	0.9077	0.920 77	0.2066	3.8	1.5617	0.652 0	0.4979
				4.0	1.6013	0.630 3	0.5337
		$Sm(NO_3)_3$		4.2	1.6399	0.608 8	0.5718
0.1	0.7424	0.994 664	0.2943	4.2774	1.6546	0.600 5	0.5871
0.2	0.7407	0.989 38	0.2453				
0.3	0.7510	0.983 89	0.2235			$Gd(NO_3)_3$	
0.4	0.7663	0.978 15	0.2117	0.1	0.7497	0.994 612	0.3002
0.5	0.7845	0.972 13	0.2050	0.2	0.7568	0.989 15	0.2545
0.6	0.8046	0.965 81	0.2015	0.3	0.7725	0.983 44	0.2349
0.7	0.8262	0.959 18	0.2001	0.4	0.7910	0.977 46	0.2247
0.8	0.8489	0.952 24	0.2003	0.5	0.8112	0.971 20	0.2193
0.9	0.8725	0.944 98	0.2017	0.6	0.8327	0.964 64	0.2169
1.0	0.8968	0.937 42	0.2042	0.7	0.8553	0.957 77	0.2166
1.2	0.9468	0.921 39	0.2115	0.8	0.8790	0.950 59	0.2178

Table III (continued)

m	ϕ	a_1	$\gamma_\pm$	m	ϕ	a_1	$\gamma_\pm$
0.9	0.9035	0.943 09	0.2204	3.2	1.6395	0.685 2	0.7292
1.0	0.9288	0.935 26	0.2241	3.4	1.6846	0.661 8	0.7941
1.2	0.9813	0.918 65	0.2342	3.6	1.7284	0.638 7	0.8638
1.4	1.0356	0.900 80	0.2475	3.8	1.7708	0.615 8	0.9385
1.6	1.0909	0.881 8	0.2638	4.0	1.8119	0.593 2	1.018
1.8	1.1467	0.861 8	0.2828	4.2	1.8519	0.570 9	1.104
2.0	1.2025	0.840 9	0.3046	4.4	1.8907	0.549 1	1.195
2.2	1.2579	0.819 2	0.3291	4.6	1.9285	0.527 7	1.292
2.4	1.3124	0.796 9	0.3563	4.8	1.9652	0.506 7	1.396
2.6	1.3660	0.774 2	0.3862	5.0	2.0010	0.486 3	1.506
2.8	1.4184	0.751 1	0.4190	5.2	2.0357	0.466 3	1.623
3.0	1.4695	0.727 8	0.4547	5.4	2.0695	0.446 9	1.746
3.2	1.5193	0.704 5	0.4933	5.6	2.1023	0.428 1	1.877
3.4	1.5675	0.681 1	0.5351	5.8	2.1341	0.409 9	2.015
3.6	1.6144	0.657 8	0.5800	6.0	2.1649	0.392 2	2.161
3.8	1.6599	0.634 7	0.6283	6.2	2.1946	0.375 1	2.314
4.0	1.7040	0.611 9	0.6800	6.4	2.2233	0.358 7	2.474
4.2	1.7469	0.589 4	0.7353	6.6	2.2508	0.342 8	2.642
4.3701	1.7824	0.570 5	0.7854	6.8	2.2771	0.327 6	2.817
				7.0	2.3022	0.313 1	2.999
		$Tb(NO_3)_3$		7.2	2.3259	0.299 2	3.186
0.1	0.7578	0.994 554	0.3033	7.2709	2.3340	0.294 4	3.254
0.2	0.7708	0.988 95	0.2606				
0.3	0.7906	0.983 05	0.2431			$Tm(NO_3)_3$	
0.4	0.8121	0.976 86	0.2346	0.1	0.7748	0.994 32	0.3095
0.5	0.8345	0.970 38	0.2306	0.2	0.7976	0.988 57	0.2726
0.6	0.8578	0.963 59	0.2295	0.3	0.8256	0.982 31	0.2596
0.7	0.8817	0.956 50	0.2303	0.4	0.8552	0.975 65	0.2554
0.8	0.9064	0.949 09	0.2328	0.5	0.8860	0.968 58	0.2558
0.9	0.9316	0.941 37	0.2364	0.6	0.9178	0.961 09	0.2594
1.0	0.9574	0.933 33	0.2412	0.7	0.9503	0.953 19	0.2652
1.2	1.0103	0.916 35	0.2535	0.8	0.9834	0.944 88	0.2729
1.4	1.0644	0.898 2	0.2691	0.9	1.0169	0.936 18	0.2822
1.6	1.1192	0.878 9	0.2877	1.0	1.0506	0.927 09	0.2929
1.8	1.1742	0.858 7	0.3093	1.2	1.1181	0.907 84	0.3182
2.0	1.2292	0.837 7	0.3338	1.4	1.1849	0.887 3	0.3481
2.2	1.2837	0.815 9	0.3612	1.6	1.2502	0.865 8	0.3826
2.4	1.3375	0.793 5	0.3916	1.8	1.3136	0.843 3	0.4213
2.6	1.3904	0.770 7	0.4251	2.0	1.3747	0.820 3	0.4644
2.8	1.4424	0.747 5	0.4618	2.2	1.4333	0.796 7	0.5117
3.0	1.4932	0.724 1	0.5018	2.4	1.4895	0.772 9	0.5635
3.2	1.5429	0.700 6	0.5453	2.6	1.5432	0.748 9	0.6196
3.4	1.5913	0.677 1	0.5923	2.8	1.5945	0.724 9	0.6803
3.6	1.6385	0.653 7	0.6431	3.0	1.6435	0.701 0	0.7457
3.8	1.6844	0.630 5	0.6978	3.2	1.6904	0.677 2	0.8158
4.0	1.7289	0.607 5	0.7566	3.4	1.7352	0.653 7	0.8909
4.2	1.7722	0.584 9	0.8195	3.6	1.7782	0.630 5	0.9712
4.4	1.8141	0.562 6	0.8866	3.8	1.8196	0.607 6	1.057
4.5320	1.8410	0.548 1	0.9334	4.0	1.8593	0.585 1	1.148
				4.2	1.8976	0.563 1	1.245
		$Er(NO_3)_3$		4.4	1.9346	0.541 5	1.348
0.1	0.7801	0.994 394	0.3078	4.6	1.9704	0.520 4	1.458
0.2	0.7983	0.988 56	0.2705	4.8	2.0051	0.499 8	1.574
0.3	0.8228	0.982 37	0.2566	5.0	2.0386	0.479 7	1.697
0.4	0.8499	0.975 80	0.2514	5.2	2.0711	0.460 2	1.827
0.5	0.8786	0.968 84	0.2510	5.4	2.1025	0.441 2	1.965
0.6	0.9084	0.961 49	0.2536	5.6	2.1329	0.422 9	2.109
0.7	0.9390	0.953 74	0.2584	5.8	2.1621	0.405 1	2.261
0.8	0.9701	0.945 61	0.2649	5.9526	2.1837	0.391 9	2.382
0.9	1.0014	0.937 12	0.2729				
1.0	1.0329	0.928 27	0.2821			$Yb(NO_3)_3$	
1.2	1.0957	0.909 60	0.3039	0.1	0.7789	0.994 403	0.3096
1.4	1.1576	0.889 8	0.3297	0.2	0.8001	0.988 53	0.2729
1.6	1.2182	0.869 0	0.3591	0.3	0.8269	0.982 28	0.2598
1.8	1.2772	0.847 3	0.3922				
2.0	1.3343	0.825 1	0.4289	0.4	0.8562	0.975 62	0.2555
2.2	1.3897	0.802 3	0.4692	0.5	0.8873	0.968 53	0.2561
2.4	1.4431	0.779 1	0.5132	0.6	0.9200	0.961 00	0.2600
2.6	1.4948	0.755 7	0.5610	0.7	0.9538	0.953 03	0.2663
2.8	1.5446	0.732 2	0.6129	0.8	0.9885	0.944 61	0.2747
3.0	1.5929	0.708 7	0.6689	0.9	1.0239	0.935 75	0.2847

Table III (continued)

m	ϕ	a_1	$\gamma_\pm$	m	ϕ	a_1	$\gamma_\pm$
1.0	1.0596	0.926 48	0.2964	4.6	2.0230	0.511 4	1.623
1.2	1.1315	0.906 79	0.3240	4.8	2.0562	0.491 0	1.754
1.4	1.2029	0.885 7	0.3570	5.0	2.0881	0.471 3	1.892
1.6	1.2729	0.863 5	0.3953	5.2	2.1187	0.452 1	2.037
1.8	1.3408	0.840 4	0.4386	5.4	2.1480	0.433 5	2.189
2.0	1.4063	0.816 5	0.4870	5.6	2.1762	0.415 5	2.349
2.2	1.4691	0.792 2	0.5407	5.8	2.2033	0.398 2	2.517
2.4	1.5290	0.767 6	0.5995	6.0	2.2293	0.381 4	2.692
2.6	1.5862	0.742 9	0.6638	6.2	2.2543	0.365 3	2.874
2.8	1.6405	0.718 2	0.7334	6.4	2.2782	0.349 7	3.065
3.0	1.6921	0.693 6	0.8086	6.6	2.3010	0.334 8	3.262
3.2	1.7411	0.669 3	0.8894	6.8	2.3227	0.320 4	3.467
3.4	1.7876	0.645 3	0.9759	7.0	2.3433	0.306 7	3.679
3.6	1.8318	0.621 8	1.068	7.2	2.3626	0.293 5	3.896
3.8	1.8738	0.598 6	1.167	7.4	2.3807	0.281 0	4.119
4.0	1.9138	0.576 0	1.271	7.6	2.3974	0.269 0	4.347
4.2	1.9519	0.553 9	1.382	7.8	2.4126	0.257 7	4.577
4.4	1.9882	0.532 4	1.500	7.9115	2.4204	0.251 6	4.707

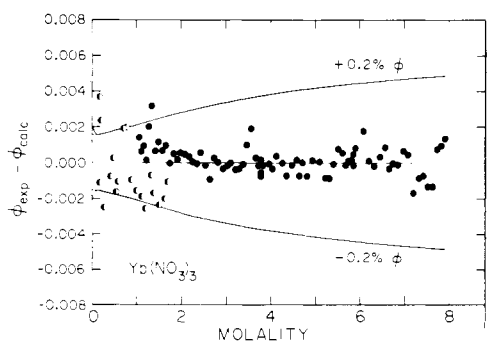

Figure 1. Differences between experimental and calculated osmotic coefficients of $Yb(NO_3)_3$ at 25 °C: O, estimated from conductances; ◐, isopiestic vs. KCl; ●, isopiestic vs. $CaCl_2$.

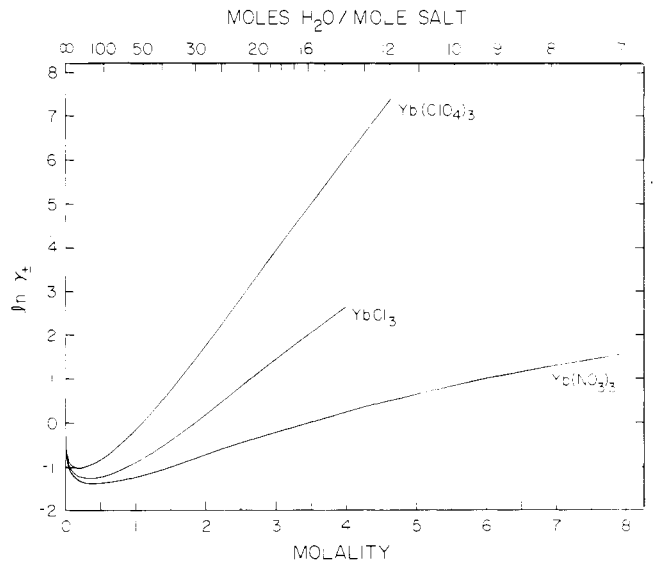

Figure 2. Natural log of the mean molal activity coefficients of $YbCl_3$, $Yb(ClO_4)_3$, and $Yb(NO_3)_3$ solutions at 25 °C.

to reflect these differences in the amount of the complex formation. This does appear to be the case (i.e., a_1 decreases from Sm to Yb at high concentrations, while ϕ and $\gamma_\pm$ increase; a_1, ϕ, and $\gamma_\pm$ are slightly out of sequence for La below 0.6 mol kg^{-1}), but additional data for other rare earth nitrates are required to confirm this deduction.

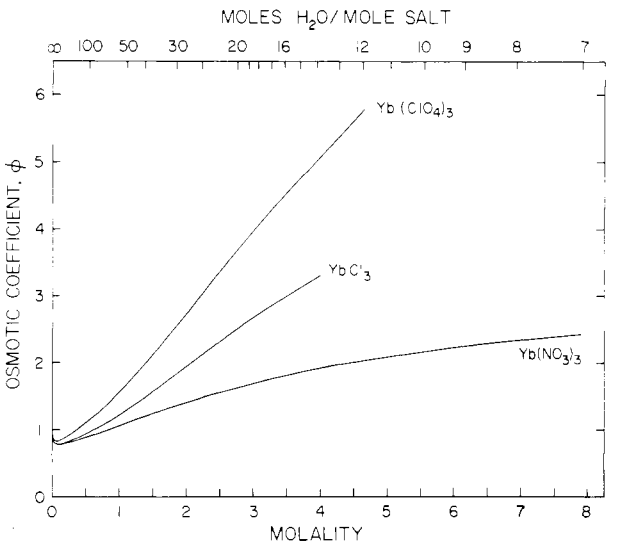

Figure 3. Osmotic coefficients of $YbCl_3$, $Yb(ClO_4)_3$, and $Yb(NO_3)_3$ solutions at 25 °C.

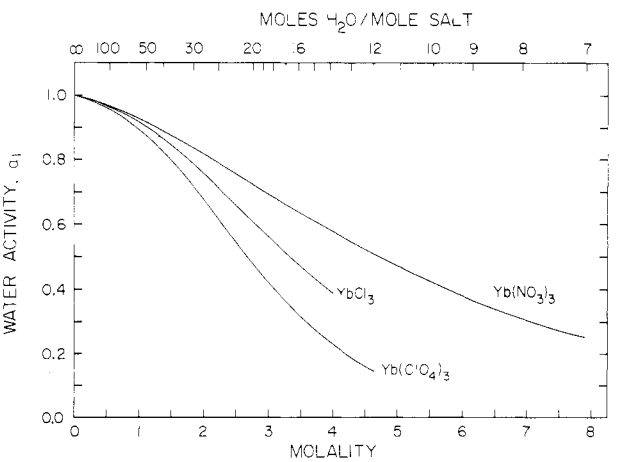

Figure 4. Water activities of $YbCl_3$, $Yb(ClO_4)_3$, and $Yb(NO_3)_3$ solutions at 25 °C.

Acknowledgments

The rare earth oxides were purified by the rare earth separation group of the Ames Laboratory. The authors thank Anton Habenschuss for assistance with the computer programming

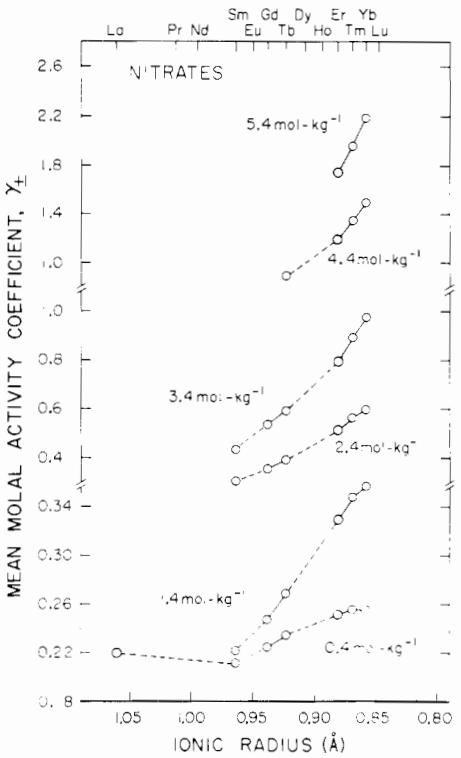

Figure 5. Mean molal activity coefficients of rare earth nitrate solutions at constant molalities.

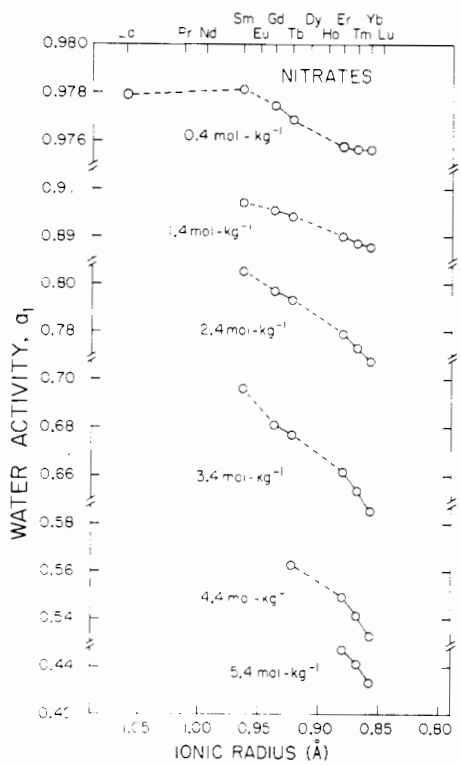

Figure 7. Water activities of rare earth nitrate solutions at constant molalities.

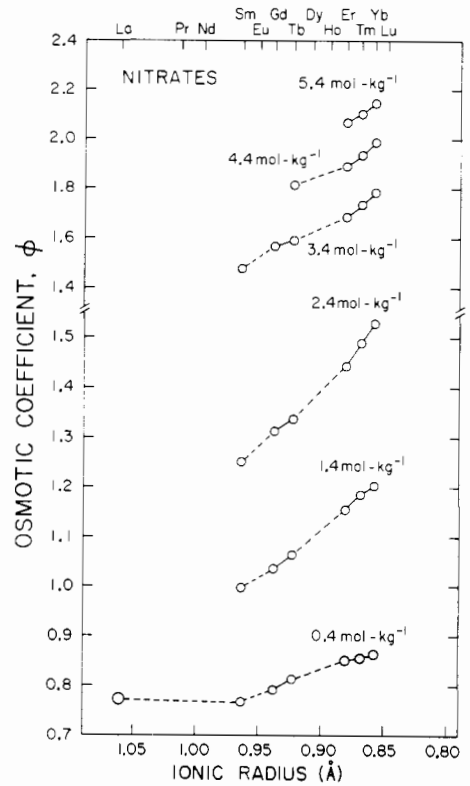

Figure 6. Osmotic coefficients of rare earth nitrate solutions at constant molalities.

and also for suggestions concerning this manuscript. In addition, the authors thank Herman O. Weber for assistance with starting the Gd, Tb, and Tm measurements.

Literature Cited

(1) Abrahamer, I., Marcus, Y., *Inorg. Chem.*, **6,** 2103 (1967).
(2) Choppin, G. R., Henrie, D. E., Buijs, K., *Inorg. Chem.*, **5,** 1743 (1966).
(3) Choppin, G. R., Strazik, W. F., *Inorg. Chem.*, **4,** 1250 (1965).
(4) Findlay, T. J. V., Symons, M. C. R., *J. Chem. Soc., Faraday Trans. 2,* **72,** 820 (1976).
(5) Garnsey, R., Ebdon, D. W., *J. Am. Chem. Soc.*, **91,** 50 (1969).
(6) Hall, R. E., Harkins, W. D., *J. Am. Chem. Soc.*, **38,** 2658 (1916).
(7) Hamer, W. J., Wu, Y.-C., *J. Phys. Chem. Ref. Data,* **1,** 1047 (1972).
(8) Heiser, D. J., unpublished Ph.D. Dissertation, Iowa State University, Ames, Iowa, 1958.
(9) Rard, J. A., Habenschuss, A., Spedding, F. H., *J. Chem. Eng. Data,* **21,** 374 (1976).
(10) Rard, J. A., Habenschuss, A., Spedding, F. H., *J. Chem. Eng. Data,* **22,** 180 (1977).
(11) Rard, J. A., Spedding, F. H., *J. Phys. Chem.*, **79,** 257 (1975).
(12) Rard, J. A., Weber, H. O., Spedding, F. H., *J. Chem. Eng. Data,* **22,** 187 (1977).
(13) Reuben, J., *J. Phys. Chem.*, **79,** 2154 (1975).
(14) Rumanova, I. M., Volodina, G. F., Belov, N. V., *Sov. Phys.-Crystallogr.* (*Engl. Transl.*) **9,** 545 (1965).
(15) Silber, H. B., Proc. 12th Rare Earth Research Conference, Vol. I, 9 (1976).
(16) Silber, H. B., Scheinin, N., Atkinson, G., Greisek, J. J., *J. Chem. Soc., Faraday Trans. 1,* **68,** 200 (1972).
(17) Spedding, F. H., Derer, J. L., Mohs, M. M., Rard, J. A., *J. Chem. Eng. Data,* **21,** 474 (1976).
(18) Spedding, F. H., Jaffe, S., *J. Am. Chem. Soc.*, **76,** 884 (1954).
(19) Spedding, F. H., Pikal, M. J., Ayers, B. O., *J. Phys. Chem.*, **70,** 2440 (1966).
(20) Spedding, F. H., Shiers, L. E., Brown, M. A., Baker, J. L., Gutierrez, L., McDowell, L. S., Habenschuss, A., *J. Phys. Chem.*, **79,** 1087 (1975).
(21) Spedding, F. H., Shiers, L. E., Rard, J. A., *J. Chem. Eng. Data,* **20,** 88 (1975).
(22) Spedding, F. H., Weber, H. O., Saeger, V. W., Petheram, H. H., Rard, J. A., Habenschuss, A., *J. Chem. Eng. Data,* **21,** 341 (1976).
(23) Templeton, D. H., Dauben, C. H., *J. Am. Chem. Soc.*, **76,** 5237 (1954).
(24) Walters, J. P., Spedding, F. H., IS-1988, unclassified A.E.C. report, Ames Laboratory, Ames, Iowa, 1968.

Received for review December 15, 1976. Accepted February 26, 1977. This work was performed for the U.S. Energy Research and Development Administration, Division of Physical Research, and is based, in part, on the Ph.D. dissertation of D. J. Heiser, Iowa State University, Ames, Iowa, 1958.